Exceptional Heat and Basin-Scale Connections in the Kuroshio-Oyashio Region in the Early 2020s

Shoshiro Minobe

minobe@sci.hokudai.ac.jp

Hokkaido University https://orcid.org/0000-0002-9487-9006

Research Article

Keywords: North Pacific, global warming, global boiling, ocean heat content

Posted Date: November 19th, 2024

DOI: https://doi.org/10.21203/rs.3.rs-5465083/v1

Additional Declarations: The authors declare no competing interests.

Abstract

This study investigates recent extreme conditions in the North Pacific, which began in the late 2010s and have intensified significantly by 2024, focusing on the Kuroshio-Oyashio region. The anomalies appear to have originated in the western North Pacific, linked to changes in the Kuroshio and Oyashio currents, while developments in the eastern North Pacific remained somewhat distinct. Sea surface temperature anomalies in the Kuroshio-Oyashio region have reached record-breaking levels, with deviations up to 6°C above the 1993–2022 average. Subsurface temperatures have also increased notably, accounting for 15.7% and 12.3% in the western and eastern North Pacific (28% combined) of the global ocean heat content increase in the 0–300 m layer between 2020s and 2010s. In the 2020s, the Kuroshio current extended northward to approximately 42°N along Japan’s coast, forming a loop-like pattern with a southward return flow, while the Kuroshio Extension in wider zonal extent also shifted northward. These oceanic anomalies are likely influenced by wind changes, with Sverdrup theory suggesting weakened subtropical gyres and a northward shift of the subtropical-subpolar gyre boundary. Further research is needed to fully understand, monitor, and predict these changes and their impacts on regional ecosystems.

Introduction

The Earth's climate has exhibited exceptional warmth from mid-2023 through the present (October 2024). This abnormal warmth is exceptional, even when considering the ongoing progression of global warming. In July 2023, the UN Secretary-General declared that the climate was no longer in a state of global warming, but instead in "global boiling."

Among the world's oceans, the Kuroshio-Oyashio (K-O) region has experienced a particularly pronounced warming during this exceptional heat period of 2023–2024. Figure 1 shows the SST anomalies for one year, from July 2023 to June 2024. In the K-O region, anomalies exceeding 6°C are observed. No other ocean region shows such high temperature anomalies. Anomalies remain below 2°C in most areas, and anomalies reaching 3°C occurred only in a narrow area of the Gulf Stream outside of the North Pacific (NP). Therefore, it can be said that the K-O region is the focal point of global boiling in 2023-24. Given the K-O region’s significant role in ocean-atmosphere interactions (Larson et al., 2024; Oka et al., 2023; Sasaki & Ito, 2024; Sato et al., 2024; Sugimoto et al., 2021) and heat transport (Kawakami et al., 2022), its investigation is of critical importance from a global perspective.

Prior to this exceptional warming in 2023–2024, several notable anomalous conditions were reported in the K-O region. In the 2010s, frequent marine heatwaves have occurred in the Kuroshio-Oyashio during the summer (Miyama et al., 2021), with the start of the MHWs being associated with the increase of fish-catch of yellow-tail in Hokkaido. The Kuroshio has been in a large meander since August 2017, which has persisted until now[1]. This is the longest period of a large meander since observations began in 1961, could be related to the oceanic circulation changes driven by anomalous atmospheric circulation (Qiu et al., 2023). The strength of the Oyashio has been decreasing according to trend analysis from 1982 to

2016 (Kawakami et al., 2024). The formation rate of the North Pacific Tropical Mode Water substantially decreased in the period 2018–2021 (Sheng et al., 2024). The North Pacific heat content increased substantially in the 2010s (Kawai et al., 2023). The marine heat wave occurred in 2020 in the northwestern Pacific (Kuroda & Setou, 2021) and in 2022–2023 in the Oyashio region, accompanied by a near surface decrease of associated abnormal Kuroshio water intrusion (Kawai et al., 2024).

Since Kuroshio and Oyashio are the western boundary currents, their variability may be related to the changes in the NP basin. In particular, Rossby waves generated in the eastern-central NP can influence the western boundary currents (Ceballos et al., 2009; Kawakami et al., 2023; Qiu, 2003; Sasaki et al., 2013; Sasaki & Schneider, 2011; Taguchi et al., 2007). Although most previous studies focused on baroclinic Rossby waves, barotropic propagation signatures associated with the Pacific Decadal Oscillation were also reported (Andres et al., 2011).

The unprecedented warming observed in 2023-24 underscores a critical need for substantial research. To start, it is essential to document recent changes in the K-O region and their relationship to variations in the NP basin. This paper aims to provide timely documentation of these exceptional conditions through analyses of observational data. A key focus of this study is to determine whether the anomalous heat in the K-O region and the broader North Pacific has significant implications for ocean heat uptake in the context of global warming. Notably, 89% of the heat accumulated by the Earth due to global warming is absorbed by the ocean (Von Schuckmann et al., 2023). Also, understanding how current changes relate to temperature shifts especially in the western NP, where narrow SST anomalies shown in Fig. 1 suggest the important roles of currents, is crucial. Given that the Kuroshio and Oyashio are wind-driven currents, this study examines the relationship between these oceanic anomalies and changes in wind forcing over the North Pacific.

The rest of the paper is organized as follows. In section 2, data and methods used in this paper are explained. In section 3, changes in temperature including ocean heat content, ocean circulation anomalies in the western NP, and the relations to atmospheric wind forcings are investigated. Summary, discussion and conclusions are given in Section 4.

[1] https://www.data.jma.go.jp/kaiyou/data/shindan/b_2/kuroshio_stream/kuroshio_stream.html (Access October 31st, 2024)

Data And Methods

In this study, the following datasets are analyzed: Optimal-Interpolation (OI) SST version 2.1 (Huang et al., 2021); The Ocean Reanalysis Version 5 (ORAS5) of European Centre for Medium-Range Weather Forecasts (ECMWF) (Zuo et al., 2019); ocean analyses of EN4.2 (Good et al., 2013), Japan Meteorological Agency (JMA) version 3.7.1 (Ishii et al., 2017), and Institute of Atmospheric Physics (IAP) in China version 4 (Cheng, Pan, et al., 2024). Satellite-derived sea-surface height (SSH) analyzed and provided by Copernicus Climate Change Service is also examined. To understand the atmospheric forcings, sea-level pressure and wind-stress of the fifth generation reanalysis dataset produced by the European Centre for Medium-Range Weather Forecasts (ECMWF) (ERA5) (Hersbach et al., 2020) is analyzed.

For the OI SST, daily data are downloaded and monthly mean from the daily data are calculated. For other data, monthly data are downloaded and analyzed. The horizontal resolution is 0.25-degree for OI-SST, satellite-derived SSH, and ERA5 data, and also ORAS5 data are around 0.25-degree on a curve-linear grid. Other data are gridded on a 1-degree grid. Climatology is calculated for a 30-year period from 1993 to 2022. Also, epoch differences between the 2020s and 2010s are calculated in some analyses.

The ocean heat content (OHC) is calculated from three-dimensional potential temperatures (ORAS5 EN4.2) or from in-situ temperatures provided by Japan Meteorological Agency (JMA) version 3.7.1 (Ishii et al., 2017) and respective salinity data using Thermodynamic Equation Of Seawater – 2010, Gibbs Seawater python package known as TEOS-10 GSW toolkit2. We also use OHC data for 0-300 m layer thickness provided by Institute of Atmospheric Physics (IAP) in China (Cheng, Abraham, et al., 2024). The heat content calculation of ORAS5 is conducted on the original native grid.

Air-sea heat fluxes are not analyzed in this paper, because a large discrepancy is found in heat fluxes among three datasets including ERA5, Japanese Reanalysis for Three Quarters of a Century (JRA3Q) (Kosaka et al., 2024) and (Modern-Era Retrospective Analysis for Research and Applications, Version 2 (MERRA2) (Gelaro et al., 2017). The large discrepancy in heat fluxes between different data products for NP variability is consistent with (Kawai et al., 2023). Recent studies by Sato et al., (2024) and Hu et al., (2024) suggested that the air-sea heat fluxes act to damp the SST anomalies in recent changes near Japan and over NP, respectively.

To understand the influence of wind forcing on ocean circulation anomalies, the Sverdrup theory is used. The meridional Sverdrup transport is given by

$$\beta V = (1/\rho) \nabla \times \boldsymbol{\tau} \quad (1)$$

where β represents the latitudinal variation of the Coriolis parameter, V is the northward transport (including both geostrophic and Ekman transports), $\boldsymbol{\tau}$ is the surface wind stress vector, and ρ is the density of seawater. When the Sverdrup transport approximation holds, characteristics of information propagation is zonal, and timescale of variability is longer than the time for propagation, the zonal integration of Sverdrup transport yields the meridional return flow at the western boundary (WB). As emphasized by Wunch (2011), the Sverdrup transport is only valid where vertical velocities in the deep ocean can be ignored. This condition does not hold well at higher latitudes Wunch (2011). Also, deviation of propagation of the Rossby wave characteristics from zonal direction is generally large in higher latitudes in baroclinic modes (e.g, Nakamura (1998)). Therefore, it is important to remain cautious of the limitations of Sverdrup theory especially in the subarctic NP.

Given the limitations of the Sverdrup theory as a coarse approximation, we use it here to examine overall tendency by combining the use of Empirical Orthogonal Function (EOF). The Sverdrup transport, as defined in Eq. (1), is calculated at each grid point using ERA5 data and integrated zonally across the North Pacific basin. The western boundary (WB) transport is assumed to be of equal magnitude but opposite in direction. This estimated WB transport is analyzed using EOF analysis, yielding a spatial pattern as a function of latitude and a corresponding temporal component. As will be shown later, several features identified in the EOF analysis of Sverdrup transport align with observed transport changes.

[2] https://teos-10.github.io/GSW-Python/ (access October 31st, 2024)

Results

3.1 Temperature Change

Let us first examine the temporal evolution in the North Pacific leading up to the sea surface temperature in Fig. 1. Figure 2 shows SST anomalies from 2010 to 2024. The last three-years (2022–2024), strong positive temperature anomalies occurred between 30°N and 50°N across the basin. These SST anomalies appear to develop from the western and eastern NP somewhat separately. SST patterns in 2020 and 2021 in the eastern NP are somewhat similar to SST anomalies of the Blob in 2015 and 2016 (Amaya et al., 2020), but recent anomalies (e.g., 2021) do not reach the North American coast as observed in 2016. Compared with SST anomalies in the eastern NP, the SST anomalies in the western NP are much more narrowly concentrated to the K-O region and the Japan Sea, clearly suggesting that ocean currents in the western NP played a role in shaping SST anomalies.

How were SST variations related to the subsurface temperature anomalies? Yearly sampled 0-300 m OHC anomalies are shown in Fig. 3. This figure indicates that the OHC anomaly development is consistent with the SST anomaly qualitatively, as positive and negative anomalies of OHC corresponding positive and negative anomalies of SST, respectively. Also, anomalies in the 2020s began to develop in western and eastern North Pacific separately in 2020. Although previous studies suggested that the jet-trapped, westward propagating Rossby waves play an important role in variability of the Kuroshio Extension (Sasaki et al., 2013; Sasaki & Schneider, 2011), westward propagating signal is not prominent in the development of the OHC anomalies in the western NP. Rather, the SST and OHC anomalies in the western NP appear to expand eastward, suggesting an important role of advection. It is interesting to note that although the OHC anomaly in the eastern NP in 2021 is somewhat similar to that in 2016 consistent with SSTs in Fig. 2, the further developments in the following years are quite different. In the 2010s, the eastern NP OHC anomalies substantially weakened in two years by 2018, but in the 2020s, strong OHC anomalies remained and merged with the OHC anomalies extending from the western NP.

The contrasting feature in the western and eastern NP is also evident in a time series comparison between area-integrated 0-300 m OHC and area-averaged SST (Fig. 4). The time series are scaled in a manner that SST and OHC anomalies in the beginning and end of the periods are comparable in the figure. In the western NP, the warmings in the late 2010s and in the 2020s are similar between SST and OHC. On the other hand, SST in the eastern NP exhibited spike-like warmings around 2015 associated with the Blob and also around 2021 in both cases without similar spikes in the OHC, which exhibits a trend-like warming from the early 2010s to present. Consequently, trend-like subsurface warming occurred in the late 2010s and 2020s both in the western and eastern NP, and additional surface warming spikes occurred in the eastern NP.

Next, we examine the global pattern of recent OHC warming to determine whether OHC warming in the NP stands out, similar to SSTs. Figure 5 shows the 0-300 m OHC difference between the periods 2020–2023 and 2010–2019. The NP exhibits the most intense warming, especially in the K-O region and the Japan Sea. The warm OHC anomalies in the central-eastern NP are related to anomalies originating from the eastern NP, as shown in Fig. 3. The pattern appears to be related to the subarctic front in the western NP and subtropical front in the eastern NP, reminiscent of SST changes that occurred in the 1940s and 1970s climatic regime shifts over the NP(Nakamura et al., 1997; Minobe & Maeda, 2005). Outside the NP, relatively strong warm anomalies are observed in the western tropical Pacific, associated with the three-year La Niña events from 2020 to 2023.

The vertical penetration of the temperature anomalies in the western and eastern NP exhibits a distinctive difference (Fig. 6). In the western NP, anomalies penetrated to deeper depths with narrower meridional distribution than in eastern NP. In the longitudinal bands 150°-160°E and 160°-170°E, meridionally narrow anomalies occur around 35°N, roughly the latitude of the Kuroshio Extension, with the maximum around 400–500 m depth. At the same time shallower anomalies occur 40°-45°N, corresponding to the subarctic frontal zone (Kida et al., 2015). The potential temperature anomalies in the eastern NP are shallower, as warmings stronger than 1C are limited to the upper 200 m depth, occupying a wide meridional extent from 30-50N.

It is informative to quantify the OHC change in each basin. Table 1 shows global and regional OHC change between 2020s (2020–2023) and 2010s (2010 – 201) in 0-300 m. The world ocean is first divided into three latitudinal bands: 20°N–90°N (referred to as the Northern Hemisphere, NH, for simplicity), 20°S–20°N (tropics), and 20°S–90°S (Southern Hemisphere, SH). Note that the areas of these three bands are uneven due to the larger land masses in the NH, as shown in the area share column. Within the NH, we further divide into sub-regions, specifically the western NP, eastern NP, and North Atlantic. Half of the global OHC change occurred in the NH, despite its area representing only a quarter of the global ocean.

Table 1

Changes in Regional and Global 0-300 m Ocean Heat Content (OHC) between the 2010s (January 2010–December 2019) and the 2020s (January 2020–December 2023). The values represent the mean OHC change derived from four data products (ORAS5, JMA version 3.7.1, EN version 4.2, and IAP version 4), with the standard deviation across these products shown in parentheses.

Area name	Area Share (%)	OHC Change (ZJ)	OHC Change Share (%)	OHC Change /Area (MJ/m^2)
Global	100.0	42.9 (3.3)	100.0 (0.0)	118 (8)
NH Mid-High Lats (20-90N)	24.6	21.6 (2.1)	50.2 (1.9)	242 (23)
Western North Pacific (20-65N, 110E-175W)	5.8	6.7 (0.8)	15.7 (1.0)	322 (37)
Eastern North Pacific (20-65N, 175W-100W)	5.7	5.3 (0.7)	12.3 (1.3)	257 (37)
North Atlantic(20-65N, 100W-30E)	8.4	8.4 (0.9)	19.5 (1.3)	274 (23)
Tropics(20S-20N)	36.5	11.6 (1.5)	27.2 (4.0)	87 (10)
SH Mid-High Lats (90S-20S)	38.4	9.6 (1.3)	22.3 (2.4)	69 (10)

The 0-300 m OHC change shares in the western NP and eastern NP are 15.7% and 12.3%, respectively, for the global OHC change (Table 1). Therefore, the NP contributed more than a quarter (28.0%) of the global ocean OHC change, despite the small area share (11.5%). The OHC change per unit area is especially strong in the western NP associated with the strong OHC changes in the K-O region. Consequently, the NP makes a substantial contribution to the global OHC change, with a notable distinction between the western and eastern NP. In the western NP, OHC changes are concentrated in a narrow region due to the influence of the K-O, while in the eastern NP, changes are spread across a wider area. If we change the depth range of evaluation from 0-300 m to 0-100 m (0-700 m), the global share of OHC change in the western and eastern Pacific increases (decreases) to 25.8% and 15.8% (10.2% and 9.9%), respectively. The NP has a larger share in the shallower depth range but remains significant within the 0-700 m depth range.

3.2 Ocean Circulation Changes in the western North Pacific

The results in the previous section indicate that the NP experienced unprecedented warming in the 2020s, not only at the surface but also in the subsurface. These subsurface temperature anomalies are likely linked to changes in ocean circulation especially in the western NP. In this section, we investigate the changes in ocean circulation in the western NP and their relationship to the SST and OHC changes documented in the previous section.

Figure 6 compares the zonal and medicinal current transport changes between 2020–2023 and 2010–2019 in the 0-300 m depth range with the SST and 0-300 m OHC changes. The northward transport anomalies are evident near the Japan coast accompanied by southward anomalies to the east. These northward and southward anomalies sandwich the high SST and OHC anomalies between them. These results suggest that the temperature advection from the Kuroshio provide the warm water anomalies, consistent with the evidence of the Kuroshio water intrusion identified by in-situ observation in this area in 2022 (Kawai et al., 2024).

The transport shows zonally extended eastward anomalies between 35°N and 37°N and westward anomalies between 33°N and 35°N between 150° and 170°E, indicating a northward migration of the Kuroshio Extension. This northward shift is associated with warm OHC anomalies and is also apparent in satellite-derived SSH data (not shown). Additional eastward transport anomalies are observed around 42°N between 150°E and 160°E, corresponding to warm SST and OHC anomalies. Consequently, the epoch differences in transport are mainly characterized by the loop-like Kuroshio northward intrusion reaching 42°N and the northward migration of the Kuroshio Extension.

To highlight some notable changes that are challenging to discern in Fig. 6c, which has been adjusted to enhance visibility of the large variations in the Kuroshio Extension, Fig. 7 shows the 0–300 m transport volume in the East China Sea and the western subarctic North Pacific. The northeastward flowing Kuroshio current in the East China Sea appears weakened, as shown by opposing southwestward anomalies. Similarly, the southwestward flowing Oyashio along the Kuril Islands is weakened. Also, in the western subarctic North Pacific, eastward transport anomalies are observed approximately along 43°N, likely associated with warm anomalies in SST and OHC seen in Fig. 6a and 6b. Unlike the northward intrusion of the Kuroshio near Japan coast and the northward shift of the Kuroshio Extension, which show corresponding changes in OI-SST, no significant SST changes accompany the observed variations in the Kuroshio in the East China Sea or in the Oyashio along the Kuril Islands. Therefore, further research is necessary to determine whether these current changes observed in ORAS5 are indeed occurring.

3.3 Wind forcings

Figure 9 shows the WB transport estimated by Sverdrup theory in combination with EOF analysis, along with the climatology of the estimated WB transport. The climatological transport reaches a maximum value of approximately 40 Sv around 30°N and decreases both northward and southward from there. To the north, it crosses zero between 40°N and 45°N, reaching about – 30 Sv at the northern boundary of the calculation region. The EOF1 pattern of Sverdrup transport shows opposite signs between the north and south, indicating that this mode generally acts to strengthen or weaken both the subtropical and subpolar circulations, though the usefulness of estimation of WB transport based on Sverdrup framework may have difficulties for subpolar gyre as described in section 2. The zero-crossing of EOF1 occurs around 34°N, nearly 10 degrees south of the climatological zero-crossing latitude. Therefore, when this mode strengthens the subtropical and subpolar circulations, it simultaneously tends to shift the circulation boundary southward; conversely, when it weakens the circulations, it tends to shift the boundary northward.

The time series for the first EOF mode (PC1) reveals pronounced anomalies in recent years. Figure 9b shows that PC1 remains generally positive after 2018, with the 5-year running mean reaching its highest value on record by the end of the period (averaged from June 2019 to July 2024). The positive PC1, combined with the spatial pattern of EOF1, suggests that this mode tends to weaken both the subtropical and subpolar gyres while shifting the gyre boundary northward in the 2020s. The northward shift of the gyre boundary is consistent with the northward migration of the Kuroshio Extension shown in Fig. 6, and the decrease of subtropical gyre is consistent with analysis by Japan Meteorological Agency (JMA). JMA publishes the transport of the Kuroshio, based on 137E repeat observation line data, and the results indicate the overall decrease from 2000 to 2023, consistent with Fig. 9b.

The temporal variability of the first EOF mode of the Sverdrup transport is closely related to the strength of the Aleutian Low, represented by the North Pacific Index (NPI), area-averaged SLP over 30-65N, 160E-140W (Trenberth & Hurrell, 1994) in Fig. 9b. The correlation coefficient between the two is 0.82 for annual raw data and 0.76 for data with a five-year moving average. However, the Aleutian Low strength exhibits a more abrupt sign reversal in the 1970s—a characteristic known as the climate regime shift (Mantua et al., 1997; Minobe, 1997, 1999). A reversal of this change occurred in the mid-2000s, during which the weakening of the Aleutian Low was also sharper than the change in PC1. Relatedly, since 2018, positive anomalies have dominated in both time series, with PC1 showing a more pronounced deviation compared to the NPI relative to pre-2000 values. Thus, while PC1 and the NPI are closely related, the regime shift-like abrupt shifts observed in the NPI are less evident in PC1. This difference is related to the fact that the PC1 deviations since 2018 are particularly large compared to those after 1970. The wind-anomalies, however, were not likely to be outstandingly unprecedented as shown in the time series, contrasting exceptional warming in SST and OHCs. Therefore, the abnormal conditions in the 2020s may be related to the wind-field change but cannot be fully explained by them.

These results suggest that the exceptional condition in the North Pacific is most likely to be related to the wind and atmospheric circulation changes over the basin. The Sverdrup transport tends to weaken the subtropical gyre and to shift the gyre boundary to the north, consistent with the observations.

Summary, Discussion and Conclusions

4.1 Summary

The present paper investigates the recent exceptional conditions in NP. The anomalous conditions started from in the late 2010s and developed rapidly to the present (2024) with signatures suggesting that the 2020s anomalous conditions originated from the western NP associated with the changes of the Kuroshio and Oyashio currents and somewhat separately from the eastern NP (Fig. 2). SST anomalies are exceptionally strong, reaching 6C for anomalies in the K-O area relative to the previous 30-years 1993–2022 (Fig. 1). Subsurface temperature also exhibits high anomalies (Fig. 3), with 28% share of 0-300 OHC warming in NP for the global ocean (Table 1). In the last three years, the Kuroshio intruded to about 42N along the Japan coast accompanied by southward return flow to just to the east of the intruding northward flow, forming a loop-like shape (Fig. 6). Also, the Kuroshio Extension shifted to the north. The anomalous condition in the North Pacific is likely to be related to the wind field change, which occurred around 2018, which can act to weaken the subtropical gyre with shifting subtropical/subpolar gyre boundary northward as suggested from Sverdrup theory (Fig. 9).

Some of the changes reported in this paper are consistent with recent publications, reinforcing their findings. Northward shifts in the Kuroshio current up to 2021 were documented by Kawakami et al. (2023), while Kawai et al. (2023) reported on OHC increase across the North Pacific up to 2020. The pronounced SST warming in the North Pacific was also examined by Hu et al. (2024). The present study places particular emphasis on analyzing the relationships among SST, ocean heat content, and ocean currents, offering a closer look at the interactions driving these changes. Additionally, by incorporating recent data through 2023–24, this study underscores the significant role of the North Pacific in contributing to global ocean heat content changes.

Since the exceptional heat in the K-O region and in the NP basin suggests that a substantial body of future studies are needed. In the following subsections, some of those opportunities are discussed.

4.2 Discussion, future opportunities

a. Can state-of-art OGCMs simulate exceptional conditions in NP in recent years?

To understand the mechanisms behind the exceptional conditions of the 2020s, numerical model simulations and experiments are highly desirable. A key first step in this direction is to assess whether the exceptional 2020s conditions can be reasonably simulated by state-of-art ocean models forced by observed boundary conditions. Recently, Kawakami et al., (2023) conducted a simulation using an eddy-resolving regional ocean model nested within a coarse-resolution global model for the period 1960–2021. Their experiment largely follows the Ocean Model Intercomparison Project Phase 2 (OMIP2) protocol (Tsujino et al., 2020) but extends the simulation period to 2021, three years beyond the standard OMIP2 endpoint of 2018.

Results from Kawakami et al. (2023) indicate a northward shift in the Kuroshio Extension (KE) latitude, along with decadal variability that aligns qualitatively with observed patterns, including consistent decadal fluctuations. However, the model somewhat underestimated the unusually rapid northward migration of the KE around 2020 (see their Fig. 2a and Fig. 7a). This raises the question of whether current state-of-the-art ocean models can adequately capture the exceptional conditions observed in the 2020s. Therefore, it is essential to compare results from other eddy-resolving ocean models to determine if the current generation of ocean models can reliably simulate these exceptional conditions in the K-O region. If OGCMs are able to replicate the 2020s conditions reasonably, further experiments should be conducted to understand the underlying mechanisms. Also, heat budget analyses should be conducted to determine where the heat came from to the North Pacific.

b. Are the exceptional conditions driven by anthropogenic influences?

An important question is whether the exceptional North Pacific conditions in the 2020s are a harbinger of global warming. It has been reported that the Kuroshio Extension shows a northward shift in observational data analyses over the past few decades. Wu et al. (2021) reported a northward trend of approximately 0.23° per decade from 1979 to 2018, while Kawakami et al. (2023) reported a trend of 0.66° per decade from 1993 to 2021.

However, projected migration of the Kuroshio Extension based on high-resolution ocean downscaling of CMIP5 climate models is estimated to range from 0.26° to 0.89° for the end of the 21st century in the RCP8.5 scenario (Nishikawa et al., 2020), smaller than the observed shift in the last few decades. The weak meridional migration is consistent with the moderate migration signatures reported by Terada & Minobe (2018), who analyzed 35 CMIP5 models. Therefore, if the climate models are reliable, it is likely that a substantial portion of the observed northward shift in the Kuroshio Extension is attributable to natural variability.

On the other hand, the reliability of climate models is under debate about the climate change pattern in the tropics and its teleconnection. Climate models generally project El Nino-like warming patterns in the tropics, but a La Niña-like trend is observed during the satellite era, which could be influenced by human activities (Watanabe et al., 2024). In association with a modeled El Niño-like warming pattern, the Aleutian Low may intensify under future global warming (Gan et al., 2017). Furthermore, if the observed La Niña-like trend is natural variability, the recent weakening of the Aleutian Low may also result from natural variability within the tropical Pacific (Capotondi et al., 2023). Therefore, further studies are needed to conclude the contribution of natural and anthropogenic origin of the observed northward Kuroshio Extension migration.

c. What is likely to occur in the coming years?

Since the North Pacific is currently storing an unusual amount of heat (Fig. 3), understanding what will happen to this heat in the coming years is crucial. It will be highly interesting to examine the predictions produced by various forecast models on this matter. Multi-year predictions are conducted within the framework of CMIP6 under the Decadal Climate Prediction Project (Boer et al., 2016), and the World Meteorological Organization, through The Lead Centre for Annual-to-Decadal Climate Prediction[3], collects data from contributing centers worldwide to summarize prediction information. Although the multi-annual predictability of the North Pacific is generally smaller than those compared to the Atlantic

(Boer et al., 2016), prediction systems that utilized high-resolution models exhibited that the Kuroshio Extension can be predicted with multi-annual lead time (Kido et al., 2023; Kim et al., 2023).

While numerical forecast simulations and analysis of their results should be addressed in a separate paper, the data examined in this study has provided intriguing insights about the near future, which I would like to share. Figure 10 shows an x-t diagram of SSH within three 5-degree north-south bands based on satellite observations. Following changes in atmospheric circulation around 2018, positive anomalies were triggered in the eastern Pacific and have since been propagating westward. The propagating positive SSH anomalies are in the central-eastern NP at the end of the record (August 2023). If this propagation continues, it is expected that the western North Pacific will experience the effects of these positive anomalies over the coming years to possibly a decade. However, it is not certain that these positive anomalies will reach the western North Pacific. Qiu (2003) suggests that the westward propagation of SSH north of the Kuroshio Extension may not penetrate into the western North Pacific.

d. Assessments of impacts on marine ecosystem

It is widely recognized that global warming and marine heatwaves have had substantial impacts on marine ecosystems (Cavole et al., 2016; Miyama et al., 2021; Yati et al., 2020). The magnitude of North Pacific heat in recent years has exceeded past levels across many regions (Fig. 1). Consequently, wide-ranging effects on marine ecosystems are expected. To fully understand the extent of these impacts, international collaboration is essential. Also, investigations about forecasting impacts on marine ecosystems should be explored (see Minobe et al., (2022) and references therein).

4.3 Conclusions

The North Pacific has exhibited exceptional heat conditions in recent years, affecting both its western and eastern regions. The significant increase in OHC highlights the North Pacific's importance in ocean heat absorption and distribution under global warming. These anomalous conditions are likely related to the weakening of the Aleutian Low and associated atmospheric circulation changes, but understanding of mechanisms is still limited. Numerous research efforts are needed in the coming years, including understanding of mechanisms, ongoing monitoring, predictions, and assessments of impacts on marine ecosystems.

[3] https://hadleyserver.metoffice.gov.uk/wmolc/ (access, Oct 31st, 2024)

Declarations

Conflict of Interest

The authors declare that they have no known financial or non-financial competing interests that could have appeared to influence the work reported in this paper.

Acknowledgement

This work was supported by the Ministry of Education, Culture, Sports, Science and Technology (MEXT) of Japan, Grant-in-Aid for Scientific Research on Innovative Areas (19H05704, 24H01502).

References

1. Amaya DJ, Miller AJ, Xie S-P, Kosaka Y (2020) Physical drivers of the summer 2019 North Pacific marine heatwave. Nature Communications, 11(1), 1903. https://doi.org/10.1038/s41467-020-15820-w
2. Andres M, Kwon Y-O, Yang J (2011) Observations of the Kuroshio's barotropic and baroclinic responses to basin-wide wind forcing. J Phys Res 116(C4):C04011. https://doi.org/10.1029/2010JC006863
3. Boer GJ, Smith DM, Cassou C, Doblas-Reyes F, Danabasoglu G, Kirtman B, Kushnir Y, Kimoto M, Meehl GA, Msadek R, Mueller WA, Taylor KE, Zwiers F, Rixen M, Ruprich-Robert Y, Eade R (2016) The Decadal Climate Prediction Project (DCPP) contribution to CMIP6. Geosci Model Dev 9(10):3751–3777. https://doi.org/10.5194/gmd-9-3751-2016
4. Capotondi A, McGregor S, McPhaden MJ, Cravatte S, Holbrook NJ, Imada Y, Sanchez SC, Sprintall J, Stuecker MF, Ummenhofer CC, Zeller M, Farneti R, Graffino G, Hu S, Karnauskas KB, Kosaka Y, Kucharski F, Mayer M, Qiu B, Xu T (2023) Mechanisms of tropical Pacific decadal variability. Nat Reviews Earth Environ 4(11):754–769. https://doi.org/10.1038/s43017-023-00486-x
5. Cavole L, Demko A, Diner R, Giddings A, Koester I, Scripps Institution of Oceanography, Pagniello, Paulsen C, Ramirez-Valdez M-L, Schwenck A, Yen S, Zill N, M., Franks P (2016) Biological Impacts of the 2013–2015 Warm-Water Anomaly in the Northeast Pacific: Winners, Losers, and the Future. Oceanography, 29(2). https://doi.org/10.5670/oceanog.2016.32
6. Ceballos LI, Di Lorenzo E, Hoyos CD, Schneider N, Taguchi B (2009) North Pacific Gyre Oscillation Synchronizes Climate Fluctuations in the Eastern and Western Boundary Systems*. J Clim 22(19):5163–5174. https://doi.org/10.1175/2009JCLI2848.1
7. Cheng L, Abraham J, Trenberth KE, Boyer T, Mann ME, Zhu J, Wang F, Yu F, Locarnini R, Fasullo J, Zheng F, Li Y, Zhang B, Wan L, Chen X, Wang D, Feng L, Song X, Liu Y, Lu Y (2024) New Record Ocean Temperatures and Related Climate Indicators in 2023. Advances in Atmospheric Sciences. https://doi.org/10.1007/s00376-024-3378-5
8. Cheng L, Pan Y, Tan Z, Zheng H, Zhu Y, Wei W, Du J, Yuan H, Li G, Ye H, Gouretski V, Li Y, Trenberth KE, Abraham J, Jin Y, Reseghetti F, Lin X, Zhang B, Chen G, Zhu J (2024) IAPv4 ocean temperature and ocean heat content gridded dataset. Earth Syst Sci Data 16(8):3517–3546. https://doi.org/10.5194/essd-16-3517-2024

9. Gan B, Wu L, Jia F, Li S, Cai W, Nakamura H, Alexander MA, Miller AJ (2017) On the Response of the Aleutian Low. https://doi.org/10.1175/JCLI-D-15-0789.1. to Greenhouse Warming
10. Gelaro R, McCarty W, Suárez MJ, Todling R, Molod A, Takacs L, Randles CA, Darmenov A, Bosilovich MG, Reichle R, Wargan K, Coy L, Cullather R, Draper C, Akella S, Buchard V, Conaty A, Da Silva AM, Gu W, Zhao B (2017) The Modern-Era Retrospective Analysis for Research and Applications, Version 2 (MERRA-2). J Clim 30(14):5419–5454. https://doi.org/10.1175/JCLI-D-16-0758.1
11. Good SA, Martin MJ, Rayner NA (2013) EN4: Quality controlled ocean temperature and salinity profiles and monthly objective analyses with uncertainty estimates. J Geophys Research: Oceans 118(12):6704–6716. https://doi.org/10.1002/2013JC009067
12. Hersbach H, Bell B, Berrisford P, Hirahara S, Horányi A, Muñoz-Sabater J, Nicolas J, Peubey C, Radu R, Schepers D, Simmons A, Soci C, Abdalla S, Abellan X, Balsamo G, Bechtold P, Biavati G, Bidlot J, Bonavita M, Thépaut J (2020) The ERA5 global reanalysis. Q J R Meteorol Soc 146(730):1999–2049. https://doi.org/10.1002/qj.3803
13. Hu Z-Z, McPhaden MJ, Huang B, Zhu J, Liu Y (2024) Accelerated warming in the North Pacific since 2013. Nat Clim Change 14(9):929–931. https://doi.org/10.1038/s41558-024-02088-x
14. Huang B, Liu C, Banzon V, Freeman E, Graham G, Hankins B, Smith T, Zhang H-M (2021) Improvements of the Daily Optimum Interpolation Sea Surface Temperature (DOISST) Version 2.1. J Clim 34(8):2923–2939. https://doi.org/10.1175/JCLI-D-20-0166.1
15. Ishii M, Fukuda Y, Hirahara S, Yasui S, Suzuki T, Sato K (2017) Sets SOLA 13(0):163–167. https://doi.org/10.2151/sola.2017-030. Accuracy of Global Upper Ocean Heat Content Estimation Expected from Present Observational Data
16. Kawai Y, Nagano A, Hasegawa T, Tomita H, Tani M (2023) Decadal changes in the basin-wide heat budget of the mid-latitude North Pacific Ocean. J Oceanogr 79(2):91–108. https://doi.org/10.1007/s10872-022-00667-0
17. Kawai Y, Oka E, Sato K, Hosoda S, Kido S (2024) Marine heatwave in the Oyashio region in 2022/23 and its impact on subsurface dissolved oxygen. J Oceanogr. https://doi.org/10.1007/s10872-024-00731-x
18. Kawakami Y, Kojima A, Murakami K, Nakano T, Sugimoto S (2022) Temporal variations of net Kuroshio transport based on a repeated hydrographic section along 137°E. Clim Dyn 59(5–6):1703–1713. https://doi.org/10.1007/s00382-021-06061-8
19. Kawakami Y, Nakano H, Urakawa LS, Toyoda T, Aoki K, Hirose N, Usui N (2024) Temporal changes of the Oyashio water distribution east of Japan under the changing climate: Development of an objective evaluation method and its application. J Oceanogr. https://doi.org/10.1007/s10872-024-00727-7
20. Kawakami Y, Nakano H, Urakawa LS, Toyoda T, Aoki K, Usui N (2023) Northward shift of the Kuroshio Extension during 1993–2021. Sci Rep 13(1):16223. https://doi.org/10.1038/s41598-023-43009-w
21. Kida S, Mitsudera H, Aoki S, Guo X, Ito S, Kobashi F, Komori N, Kubokawa A, Miyama T, Morie R, Nakamura H, Nakamura T, Nakano H, Nishigaki H, Nonaka M, Sasaki H, Sasaki YN, Suga T, Sugimoto

S, Usui N (2015) Oceanic fronts and jets around Japan: A review. J Oceanogr 71(5):469–497. https://doi.org/10.1007/s10872-015-0283-7

22. Kido S, Nonaka M, Miyazawa Y (2023) Skillful Multiyear Prediction of the Kuroshio and Gulf Stream Jets and Eddy Activity. Geophys Res Lett 50(15). https://doi.org/10.1029/2023GL103705. e2023GL103705
23. Kim WM, Yeager SG, Danabasoglu G, Chang P (2023) Exceptional multi-year prediction skill of the Kuroshio Extension in the CESM high-resolution decadal prediction system. Npj Clim Atmospheric Sci 6(1):118. https://doi.org/10.1038/s41612-023-00444-w
24. Kosaka Y, Kobayashi S, Harada Y, Kobayashi C, Naoe H, Yoshimoto K, Harada M, Goto N, Chiba J, Miyaoka K, Sekiguchi R, Deushi M, Kamahori H, Nakaegawa T, Tanaka TY, Tokuhiro T, Sato Y, Matsushita Y, Onogi K (2024) The JRA-3Q Reanalysis. J Meteorological Soc Japan Ser II 102(1):49–109. https://doi.org/10.2151/jmsj.2024-004
25. Kuroda H, Setou T (2021) Extensive Marine Heatwaves at the Sea Surface in the Northwestern Pacific Ocean in Summer 2021. Remote Sens 13(19):3989. https://doi.org/10.3390/rs13193989
26. Larson JG, Thompson DWJ, Hurrell JW (2024) Signature of the western boundary currents in local climate variability. Nature 634(8035):862–867. https://doi.org/10.1038/s41586-024-08019-2
27. Mantua NJ, Hare SR, Zhang Y, Wallace JM, Francis RC (1997) A Pacific Interdecadal Climate Oscillation with Impacts on Salmon Production. Bull Am Meteorol Soc 78(6):1069–1079. https://doi.org/10.1175/1520-0477(1997)078<1069:APICOW>2.0.CO;2
28. Minobe S (1997) A 50–70 year climatic oscillation over the North Pacific and North America. Geophys Res Lett 24(6):683–686. https://doi.org/10.1029/97GL00504
29. Minobe S (1999) Resonance in bidecadal and pentadecadal climate oscillations over the North Pacific: Role in climatic regime shifts. Geophys Res Lett 26(7):855–858. https://doi.org/10.1029/1999GL900119
30. Minobe S, Capotondi A, Jacox MG, Nonaka M, Rykaczewski RR (2022) Toward Regional Marine Ecological Forecasting Using Global Climate Model Predictions From Subseasonal to Decadal Timescales: Bottlenecks and Recommendations. Front Mar Sci 9:855965. https://doi.org/10.3389/fmars.2022.855965
31. Minobe S, Maeda A (2005) A 1° monthly gridded sea-surface temperature dataset compiled from ICOADS from 1850 to 2002 and Northern Hemisphere frontal variability. Int J Climatol 25(7):881–894. https://doi.org/10.1002/joc.1170
32. Miyama T, Minobe S, Goto H (2021) Marine Heatwave of Sea Surface Temperature of the Oyashio Region in Summer in 2010–2016. Front Mar Sci 7:576240. https://doi.org/10.3389/fmars.2020.576240
33. Nakamura H (1998) Simple Model Prediction of Horizontal Temperature Fields in the Subtropical–Subpolar System Caused by Sudden Change in Wind Stress Curl. J Phys Oceanogr 28(8):1578–1597. https://doi.org/10.1175/1520-0485(1998)028<1578:SMPOHT>2.0.CO;2

34. Nakamura H, Lin G, Yamagata T (1997) Decadal Climate Variability in the North Pacific during the Recent Decades. Bull Am Meteorol Soc 78(10):2215–2225. https://doi.org/10.1175/1520-0477(1997)078<2215:DCVITN>2.0.CO;2
35. Nishikawa H, Nishikawa S, Ishizaki H, Wakamatsu T, Ishikawa Y (2020) Detection of the Oyashio and Kuroshio fronts under the projected climate change in the 21st century. Progress Earth Planet Sci 7(1). Article 1. https://doi.org/10.1186/s40645-020-00342-2
36. Oka E, Sugimoto S, Kobashi F, Nishikawa H, Kanada S, Nasuno T, Kawamura R, Nonaka M (2023) Subtropical Mode Water south of Japan impacts typhoon intensity. Sci Adv 9(37):eadi2793. https://doi.org/10.1126/sciadv.adi2793
37. Qiu B (2003) Kuroshio Extension Variability and Forcing of the Pacific Decadal Oscillations: Responses and Potential Feedback. J Phys Oceanogr 33(12):2465–2482. https://doi.org/10.1175/1520-0485(2003)033<2465:KEVAFO>2.0.CO;2
38. Qiu B, Chen S, Oka E (2023) Why Did the 2017 Kuroshio Large Meander Event Become the Longest in the Past 70 Years? Geophys Res Lett 50(10). https://doi.org/10.1029/2023GL103548. e2023GL103548
39. Sasaki YN, Ito R (2024) Impact of the Kuroshio large meander on local atmospheric circulation and precipitation in winter. Progress Earth Planet Sci 11(1):15. https://doi.org/10.1186/s40645-024-00620-3
40. Sasaki YN, Minobe S, Schneider N (2013) Decadal Response of the Kuroshio Extension Jet to Rossby Waves: Observation and Thin-Jet Theory*. J Phys Oceanogr 43(2):442–456. https://doi.org/10.1175/JPO-D-12-096.1
41. Sasaki YN, Schneider N (2011) Decadal Shifts of the Kuroshio Extension Jet: Application of Thin-Jet Theory*. J Phys Oceanogr 41(5):979–993. https://doi.org/10.1175/2010JPO4550.1
42. Sato H, Takemura K, Ito A, Umeda T, Maeda S, Tanimoto Y, Nonaka M, Nakamura H (2024) Impact of an unprecedented marine heatwave on extremely hot summer over Northern Japan in 2023. Sci Rep 14(1):16100. https://doi.org/10.1038/s41598-024-65291-y
43. Sheng J, Liu C, Gu Y, Li P, Zhai F, Zhou N (2024) Anomalous North Pacific subtropical mode water volume and density decrease in a recent stable Kuroshio Extension period from Argo observations. Ocean Sci 20(3):817–834. https://doi.org/10.5194/os-20-817-2024
44. Sugimoto S, Qiu B, Schneider N (2021) Local Atmospheric Response to the Kuroshio Large Meander Path in Summer and Its Remote Influence on the Climate of Japan. J Clim 34(9):3571–3589. https://doi.org/10.1175/JCLI-D-20-0387.1
45. Taguchi B, Xie S-P, Schneider N, Nonaka M, Sasaki H, Sasai Y (2007) Decadal Variability of the Kuroshio Extension: Observations and an Eddy-Resolving Model Hindcast*. J Clim 20(11):2357–2377. https://doi.org/10.1175/JCLI4142.1
46. Terada M, Minobe S (2018) Projected sea level rise, gyre circulation and water mass formation in the western North Pacific: CMIP5 inter-model analysis. Clim Dyn 50(11–12):4767–4782. https://doi.org/10.1007/s00382-017-3902-8

47. Trenberth KE, Hurrell JW (1994) Decadal atmosphere-ocean variations in the Pacific. Clim Dyn 9(6):303–319. https://doi.org/10.1007/BF00204745
48. Tsujino H, Urakawa LS, Griffies SM, Danabasoglu G, Adcroft AJ, Amaral AE, Arsouze T, Bentsen M, Bernardello R, Böning CW, Bozec A, Chassignet EP, Danilov S, Dussin R, Exarchou E, Fogli PG, Fox-Kemper B, Guo C, Ilicak M, Yu Z (2020) Evaluation of global ocean–sea-ice model simulations based on the experimental protocols of the Ocean Model Intercomparison Project phase 2 (OMIP-2). Geosci Model Dev 13(8):3643–3708. https://doi.org/10.5194/gmd-13-3643-2020
49. Von Schuckmann K, Minière A, Gues F, Cuesta-Valero FJ, Kirchengast G, Adusumilli S, Straneo F, Ablain M, Allan RP, Barker PM, Beltrami H, Blazquez A, Boyer T, Cheng L, Church J, Desbruyeres D, Dolman H, Domingues CM, García-García A, Zemp M (2023) Heat stored in the Earth system 1960–2020: Where does the energy go? Earth Syst Sci Data 15(4):1675–1709. https://doi.org/10.5194/essd-15-1675-2023
50. Watanabe M, Kang SM, Collins M, Hwang Y-T, McGregor S, Stuecker MF (2024) Possible shift in controls of the tropical Pacific surface warming pattern. Nature 630(8016):315–324. https://doi.org/10.1038/s41586-024-07452-7
51. Wu B, Lin X, Yu L (2021) Poleward Shift of the Kuroshio Extension Front and Its Impact on the North Pacific Subtropical Mode Water in the Recent Decades. J Phys Oceanogr 51(2):457–474. https://doi.org/10.1175/JPO-D-20-0088.1
52. Wunsch C (2011) The decadal mean ocean circulation and Sverdrup balance. J Mar Res 69:417–434[4]
53. Yati E, Minobe S, Mantua N, Ito S, Di Lorenzo E (2020) Marine Ecosystem Variations Over the North Pacific and Their Linkage to Large-Scale Climate Variability and Change. Front Mar Sci 7:578165. https://doi.org/10.3389/fmars.2020.578165
54. Zuo H, Balmaseda MA, Tietsche S, Mogensen K, Mayer M (2019) The ECMWF operational ensemble reanalysis–analysis system for ocean and sea ice: A description of the system and assessment. Ocean Sci 15(3):779–808. https://doi.org/10.5194/os-15-779-2019

[4] available at http://ocean.mit.edu/~cwunsch/papersonline/sverdrup_balance_jmr2011.pdf (Oct 31stt, 2024 access)

Figures

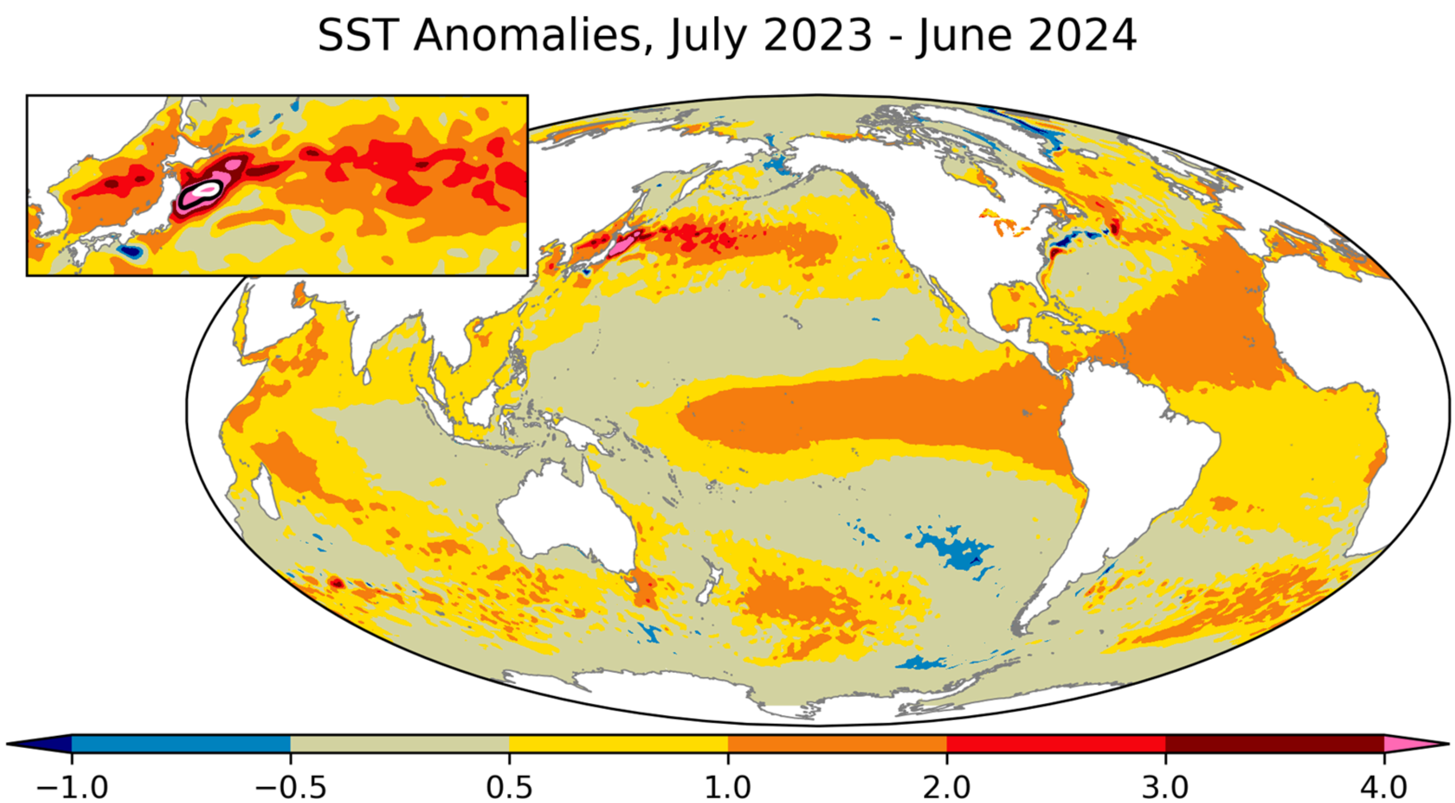

Figure 1

SST anomalies averaged from July 2023 to June 2024, relative to climatology for 1993-2022 period. The black and white contours in the inset show 5 and 6C anomalies.

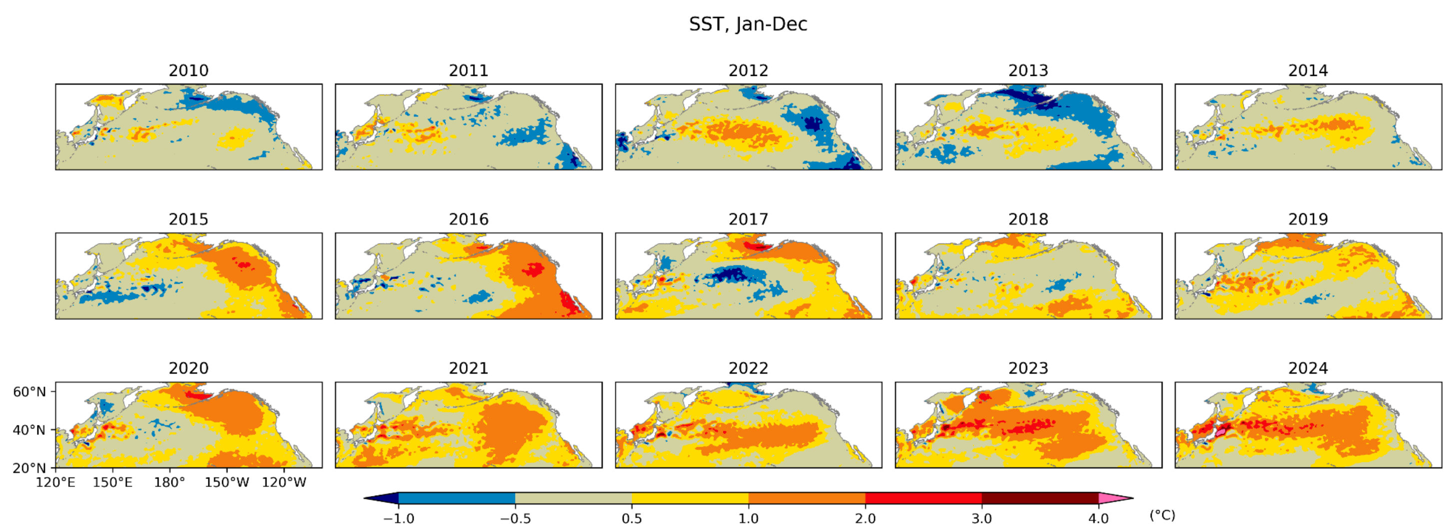

Figure 2

Annually averaged SST anomalies from 2010 to 2024. The anomalies are averaged from January to December in respective years.

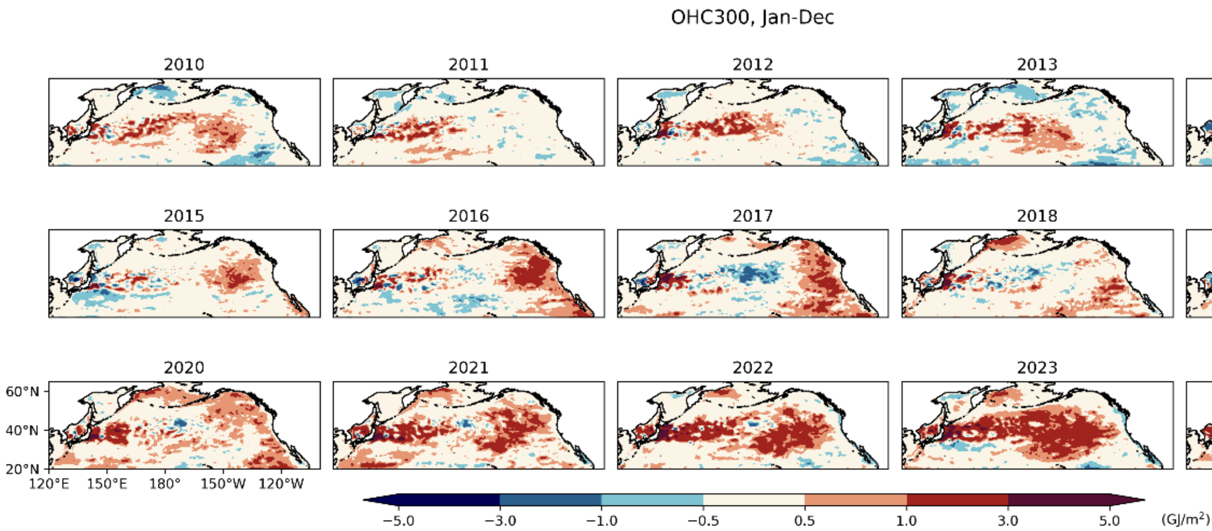

Figure 3

Same as Fig. 2, but for 0-300 m OHC per unit area.

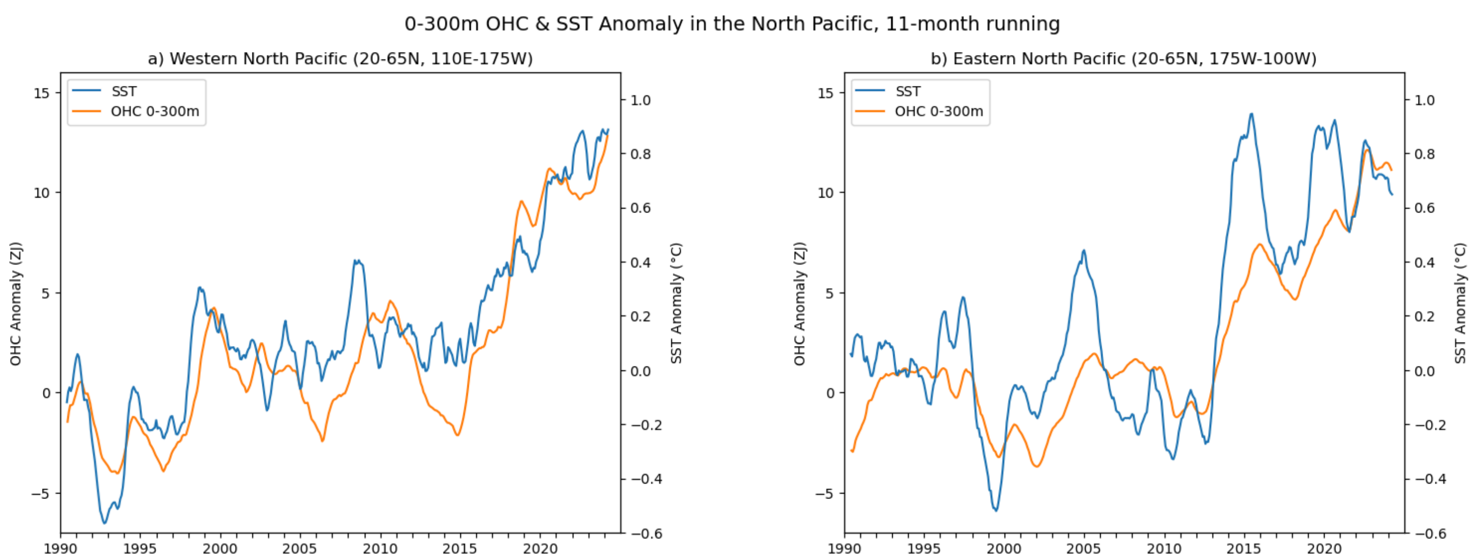

Figure 4

Area averaged SST anomaly and area-integrated 0-300 m OHC anomaly over (a) the western North Pacific, and (b) eastern North Pacific. Anomalies are calculated relative to 1993-2022 and are smoothed by 11-month running mean.

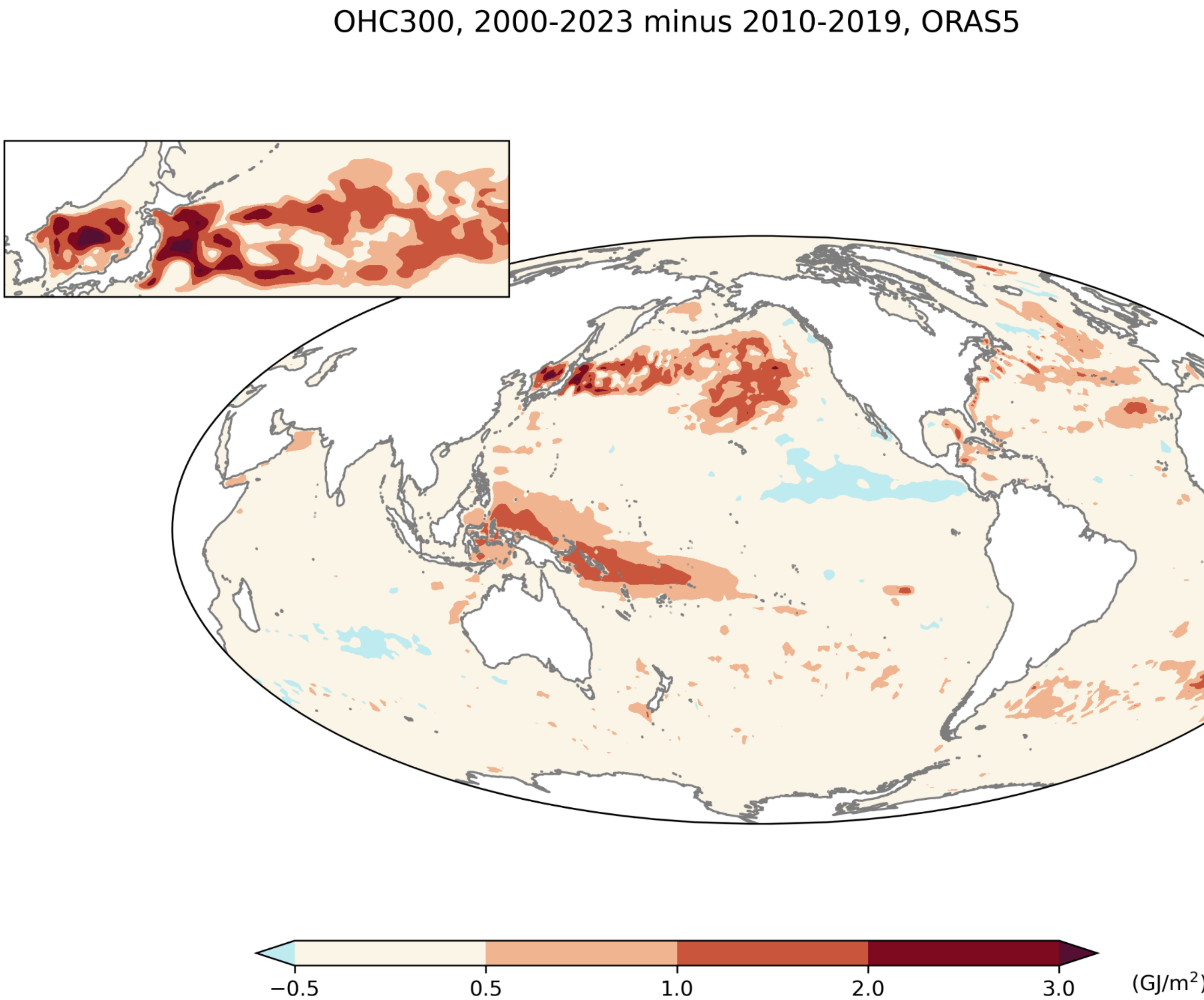

Figure 5

Difference of 0-300 m OHC per unit area in ORAS5 between 2000-2023 and 2010-2019 periods.

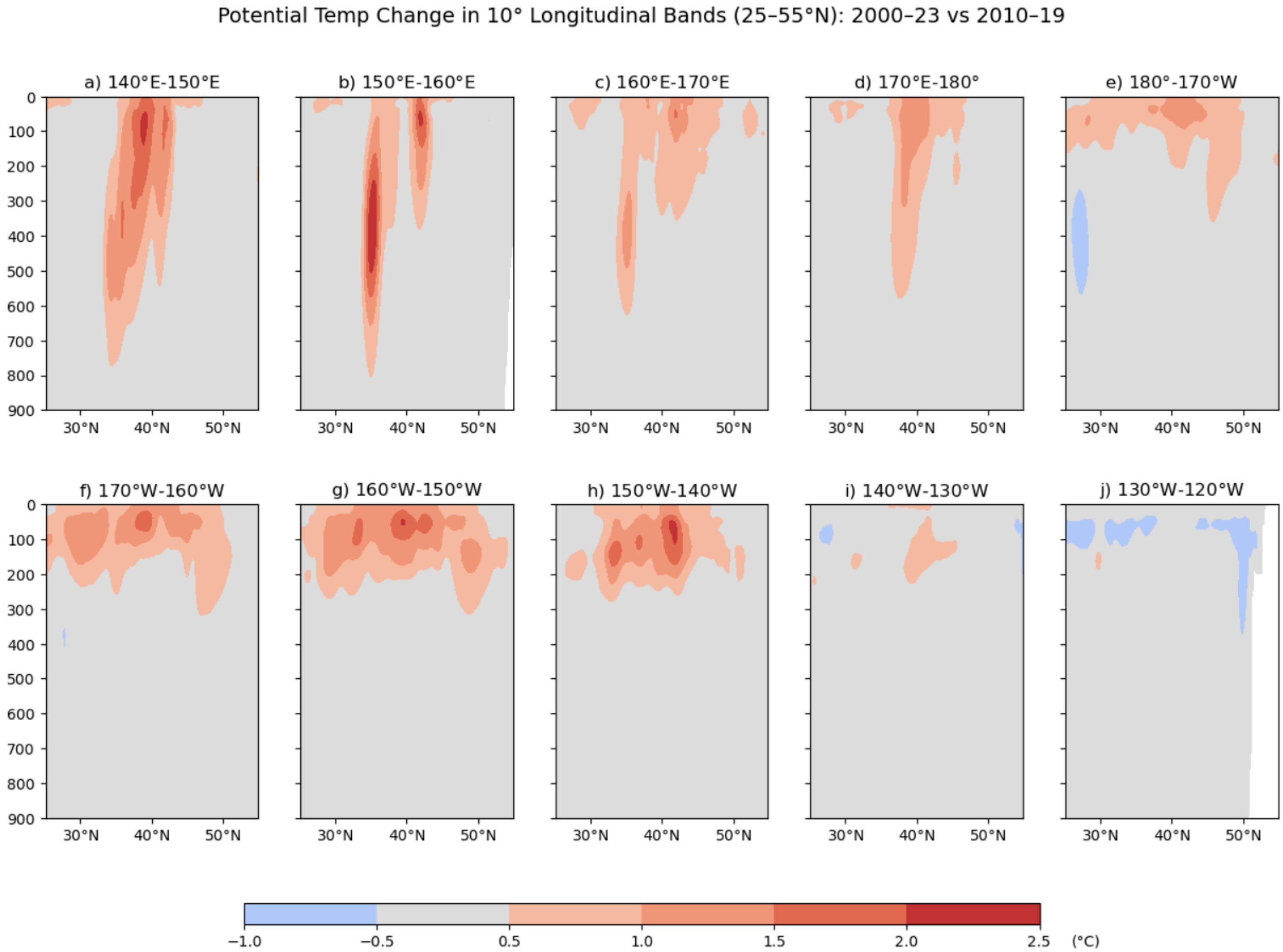

Figure 6

Difference of potential temperature in 10-degree zonal bands in ORAS5 between 2000-2023 and 2010-2019 periods.

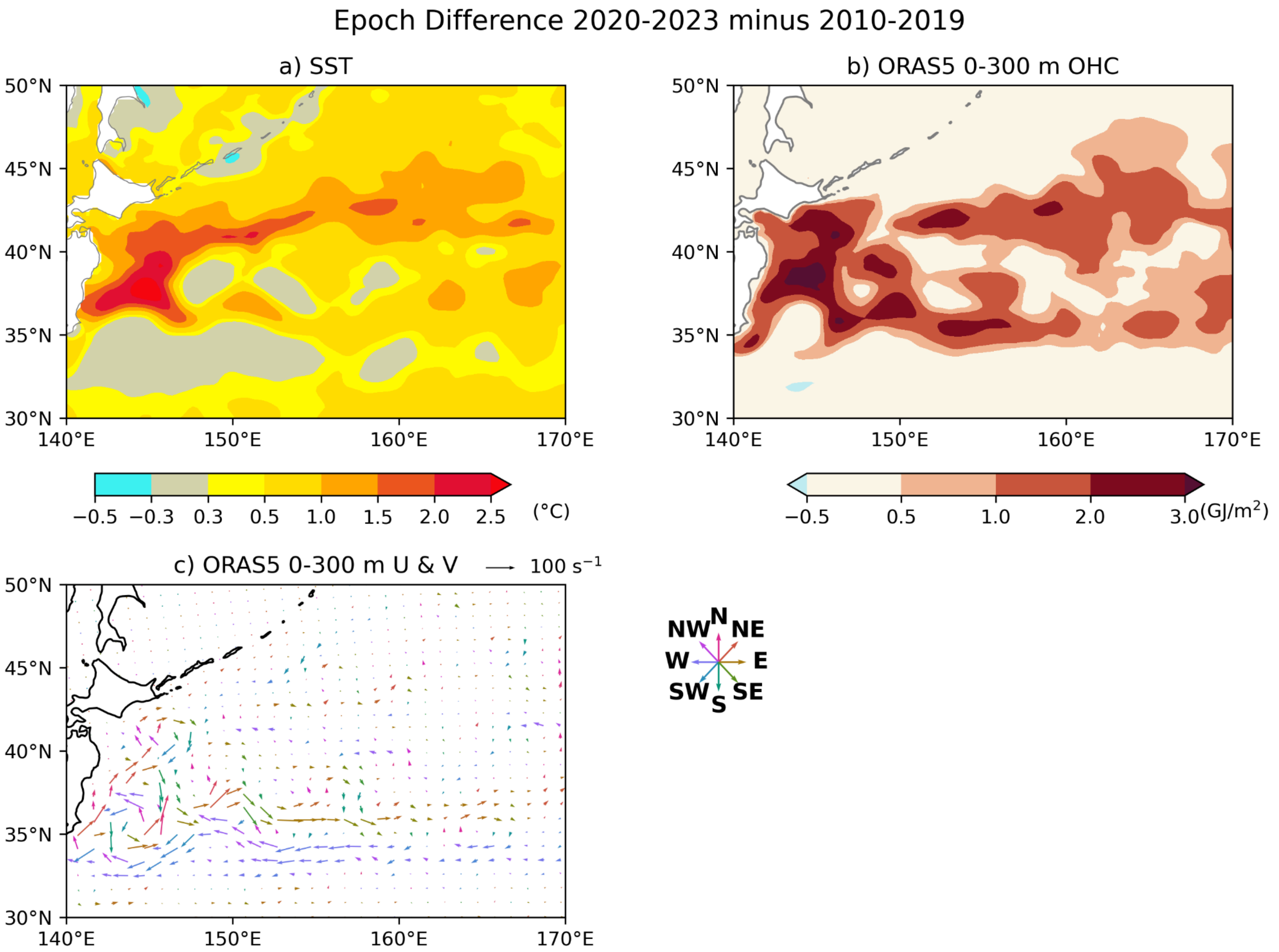

Figure 7

Differences of (a) SST, (b) 0-300 m OHC, and (c) 0-300m ocean transport between 2020-2023 and 2010-2019 periods. Colors in panel (c) indicate the directions of the transport as shown by the reference arrows to the right of the panel.

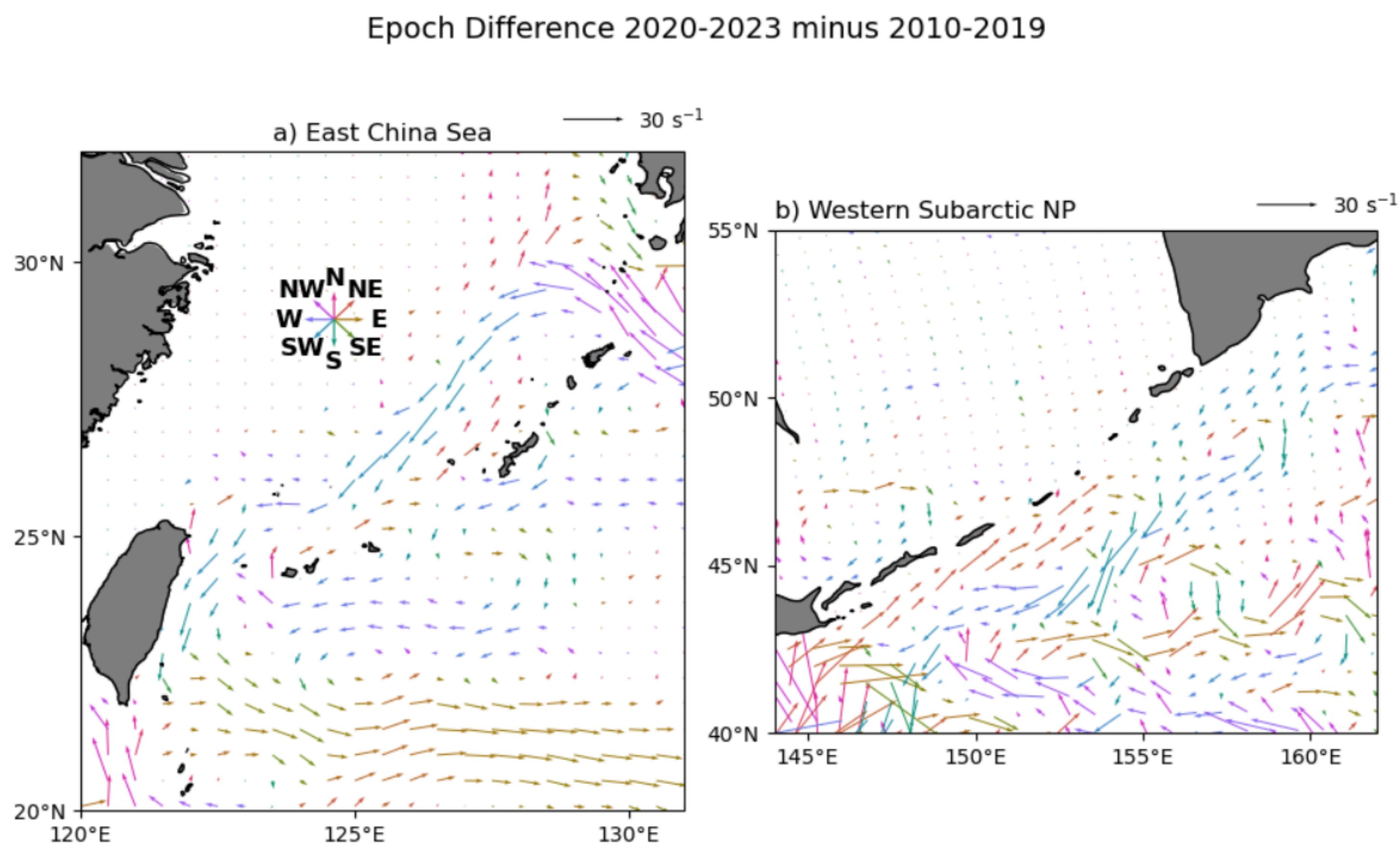

Figure 8

Same as Fig. 7c, but for (a) East China Sea, and (b) western subarctic NP.

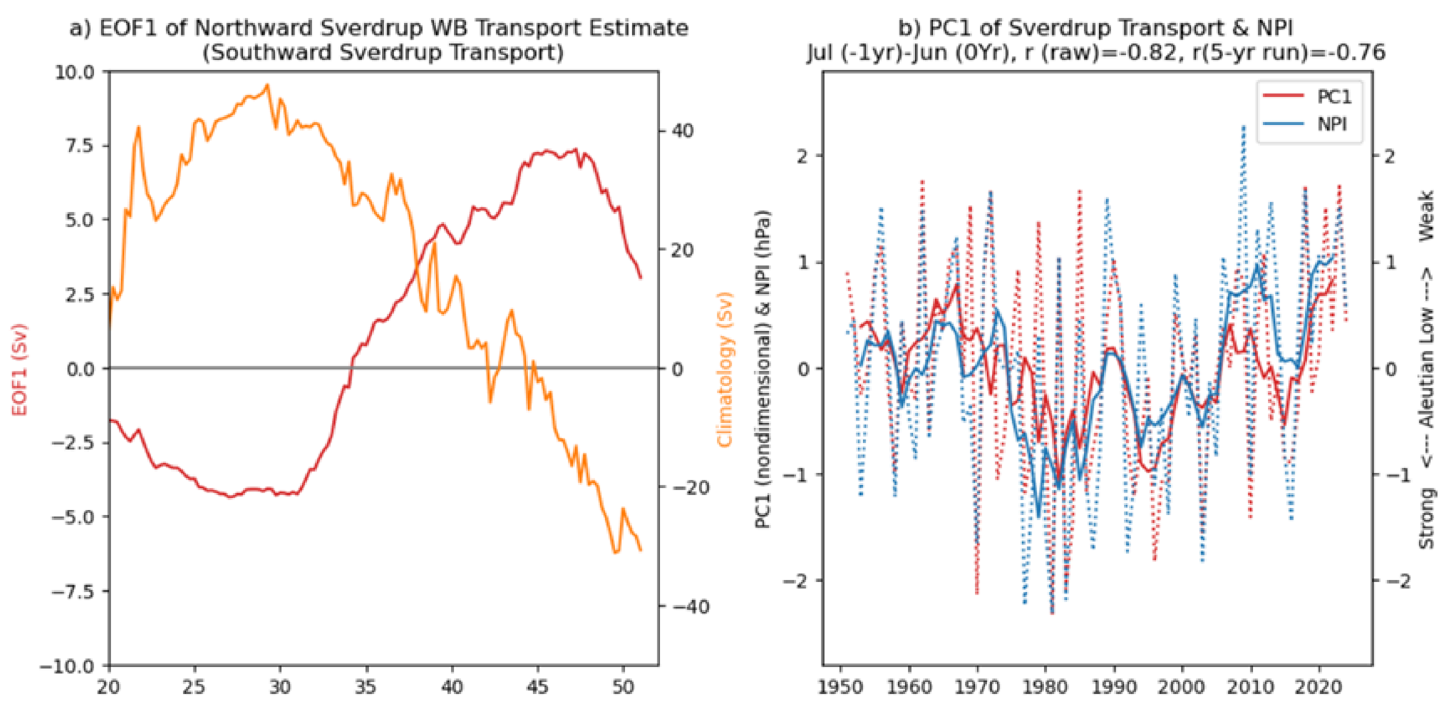

Figure 9

Northward WB transport estimated from Sverdrup theory, showing both climatology and variability represented by the first EOF mode. (a) The climatological mean northward WB transport is shown by the yellow curve, and the spatial pattern of EOF1 for WB transport is shown by the red curve. (b) Temporal variability of the EOF1 mode (PC1) is shown by the red curve, with the NPI displayed by the blue curve. In panel (b), yearly sampled raw data (averaged from July of the previous year to June of the current year) is shown by the dashed line, while the 5-year running average is shown by the solid line. Before calculating the EOF, the transport is averaged from July of one year to June of the following year, with the year shown in the figure corresponding to the latter year.

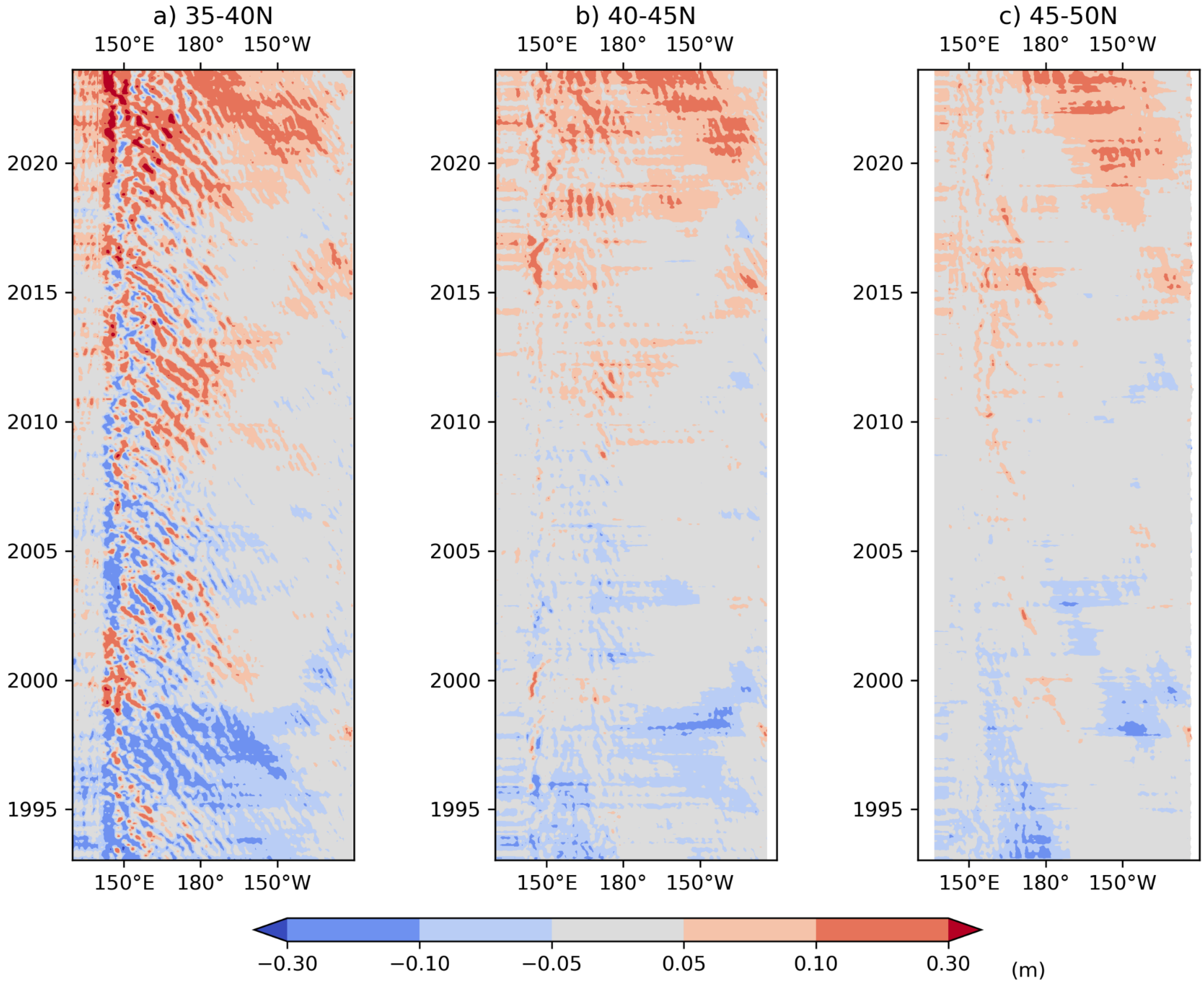

Figure 10

X-t diagram of satellite-derived SSH anomalies between (a) 35-40N, (b) 40-45N, and (c) 45-50N. Reference period is calculated from 1993 to 2022.